ISSN 1674-1056
http://cpb.iphy.ac.cn
http://iopscience.iop.org/cpb
中国物理 B
Chinese Physics
中国物理
Chinese Physics B

Attosecond transient absorption spectroscopy:Comparative study based on three-level modeling

Zeng-Qiang Yang(杨增强), Di-Fa Ye(叶地发), Li-Bin Fu(傅立斌)
Citation: Chin. Phys. B . 2018, 27(1): 013301. **doi:** 10.1088/1674-1056/27/1/013301

Journal homepage: http://cpb.iphy.ac.cn; http://iopscience.iop.org/cpb

What follows is a list of articles you may be interested in

Polarization control of multi-photon absorption under intermediate femtosecond laser field

Wenjing Cheng(程文静), Pei Liu(刘沛), Guo Liang(梁果), Ping Wu(吴萍), Tianqing Jia(贾天卿), Zhenrong Sun(孙真荣), Shian Zhang(张诗按)
Chin. Phys. B . 2017, 26(8): 083201. **doi:** 10.1088/1674-1056/26/8/083201

Frequency dependence of quantum path interference in non-collinear high-order harmonic generation

Shi-Yang Zhong(钟诗阳), Xin-Kui He(贺新奎), Hao Teng(滕浩), Peng Ye(叶蓬), Li-Feng Wang(汪礼锋), Peng He(何鹏), Zhi-Yi Wei(魏志义)
Chin. Phys. B . 2016, 25(2): 023301. **doi:** 10.1088/1674-1056/25/2/023301

Field ionization process of Eu $4f^7 6snp$ Rydberg states

Zhang Jing, Shen Li, Dai Chang-Jian
Chin. Phys. B . 2015, 24(11): 113201. **doi:** 10.1088/1674-1056/24/11/113201

Quantum path control using attosecond pulse trains via UV-assisted resonance enhance ionization

Li Fang, Wei Lai, He Zhi-Cong
Chin. Phys. B . 2015, 24(4): 043301. **doi:** 10.1088/1674-1056/24/4/043301

Precision frequency measurement of $^1S_0$-$^3P_1$ intercombination lines of Sr isotopes

Liu Hui, Gao Feng, Wang Ye-Bing, Tian Xiao, Ren Jie, Lu Ben-Quan, Xu Qin-Fang, Xie Yu-Lin, Chang Hong
Chin. Phys. B . 2015, 24(1): 013201. **doi:** 10.1088/1674-1056/24/1/013201

Attosecond transient absorption spectroscopy: Comparative study based on three-level modeling*

Zeng-Qiang Yang(杨增强)[1,†], Di-Fa Ye(叶地发)[1], and Li-Bin Fu(傅立斌)[1,2,3,‡]

[1] *Institute of Applied Physics and Computational Mathematics, Beijing* 100088, *China*
[2] *CAPT, HEDPS, and IFSA Collaborative Innovation Center of MoE, Peking University, Beijing* 100871, *China*
[3] *Center for Fusion Energy Science and Technology, China Academy of Engineering Physics, Beijing* 100088, *China*

(Received 14 June 2017; revised manuscript received 11 October 2017; published online 22 December 2017)

In the present paper, the time-resolved transient absorption spectroscopy of helium atoms is investigated based on the three-level modeling. The helium atoms are subjected to an extreme ultraviolet (XUV) attosecond pulse and a time-delayed infrared (IR) few-cycle laser field. The odd excited state are populated from the ground state by the XUV pulse due to the dipole selection rule, and probed by the time-delayed IR laser. The time-resolved transient absorption spectroscopy based on the different coupling mechanism demonstrate some different features, the photoabsorption spectrum based on three-level model with rotating wave approximation (RWA) cannot repeat the fast oscillation and the sideband structure which have been observed in the previous experimental investigation. The dressing effect of IR laser pulse on the ground state can contribute new interference structures in the photoabsorption spectrum.

Keywords: extreme ultraviolet (XUV), photoabsorption, time delay, three-level model

PACS: 33.20.Xx, 32.30.Jc, 32.80.Qk, 32.80.Wr **DOI:** 10.1088/1674-1056/27/1/013301

1. Introduction

In the last decade, attosecond technology has made great progresses which have offered much opportunities for the investigation of the time-resolved dynamics of electrons in atoms and molecules.[1–3] In general, an attosecond pulsed XUV light together with a synchronized infrared (IR) laser pulse is employed to shine on atoms or molecules, and then measure the photoions, photoelectrons, or the XUV photoabsorption spectrum. Especially, attosecond transient XUV absorption spectroscopy[4–6] explores a delay-dependent pump-probe scheme to investigate ultrafast electron dynamics down to the subfemtosecond time scale, which provides very high precision control of the delay time between them. Information on the time-resolved dynamics can be extracted by adjusting the time delay between the XUV and the IR pulses.

Recently, much effort has been made on the transient absorption spectrum.[7–22] It is demonstrated that attosecond absorption spectrum varies as a function of the IR laser intensity and the XUV-IR time delay. The shifting, splitting and broadening of main absorption lines were observed, new IR laser-induced absorption structures corresponding to multiphoton excitation of dipole-forbidden transitions were also observed.[13–15] Even several new features of subcycle oscillations resulted from quantum interferences from different multiphoton excitation pathways were observed in the transient absorption spectroscopy.[12] Furthermore, Fano profile[23] has been observed in several attosecond absorption spectrum studies carried for the doubly-excited states,[16–21] resonance line shapes can be converted among the symmetric Lorentz, regular Fano, and inverted Fano shapes in the presence of a time-delayed IR laser field.

For recent experimental research, *ab initio* solutions of the time-dependent Schrödinger equation (TDSE) have also been obtained. However, it is demonstrated that it is difficult to do full numerical simulation and understand attosecond transient absorption spectrum (ATAS) experiments from intuitive physics.[19] For this reason, most experiments were interpreted more generally by exploring a three-level model or other simplified systems to explain the dominant features of the experiments.[12,17,22] However, it is unclear whether the three-level model employed in the most studies can fully reproduce the full information of the transient absorption spectrum, and what is the differences between them. These considerations motivate the current work. In this paper, by employing three different kinds of three-level models, we investigate the attosecond transient absorption spectroscopy of helium atoms and comparing among them. In our study, the excited states are populated by a single attosecond XUV pulse. We study the initiated wave-packet oscillations under the influence of a moderately strong IR laser pulse with a controlled time delay with respect to the XUV pump pulse, which transiently induces spectral modifications and compare among different modeling.

*Project supported by the National Natural Science Foundation of China (Grant Nos. 11674034 and 11564033) and the Foundation of President of the China Academy of Engineering Physics (Grant No. 2014-1-029).

†Corresponding author. E-mail: yangzq@ymail.com
‡Corresponding author. E-mail: lbfu@iapcm.ac.cn

© 2018 Chinese Physical Society and IOP Publishing Ltd

The paper is structured as follows. Section 2 is our theoretical models. The main results are presented and discussed in Section 3. We draw our conclusions in Section 4. Atomic units (a.u.) are used throughout the paper unless otherwise specified.

2. Theoretical method

2.1. Three-level models

In the present paper, we choose the central frequency of the attosecond XUV pulse in the vicinity of the singly excited states of the helium atom and well below the doubly excited states, thus the well-known single-active-electron (SAE) approximation is valid. Under this assumption, the time-dependent Schrödinger equation (TDSE), in the length gauge with dipole approximation, can be written as

$$\mathrm{i}\frac{\partial \Psi(t)}{\partial t} = [H_0 + \boldsymbol{r}\cdot\boldsymbol{E}(t)]\Psi(t), \tag{1}$$

where $H_0 = -\frac{1}{2}\nabla^2 - 1/\boldsymbol{r}$ is the Hamiltonian of the system itself, $\boldsymbol{r}$ is the coordinate of the electron. The external field $\boldsymbol{E}(t)$ is a superposition of an XUV pulse $\boldsymbol{E}_X(t,t_\mathrm{d})$ and an IR laser pulse $\boldsymbol{E}_\mathrm{L}(t)$. The pulses are linearly polarized in the same direction and defined by

$$E_\mathrm{X}(t,t_\mathrm{d}) = E_{\mathrm{X}0}\,\mathrm{e}^{-(2\ln 2)[(t+t_\mathrm{d})/\tau_\mathrm{X}]^2}\cos\omega_\mathrm{X}(t+t_\mathrm{d}), \tag{2}$$

$$E_\mathrm{L}(t) = \begin{cases} 0, & \text{if} \quad |t| \geqslant \tau_\mathrm{L}/2 \\ E_{\mathrm{L}0} f(t)\cos\omega_\mathrm{L} t, & \text{otherwise}, \end{cases} \tag{3}$$

respectively. Here, $f(t) = \cos^2(\pi t/\tau_\mathrm{L})$ is the IR laser profile, $E_{\mathrm{X}0}$ and $E_{\mathrm{L}0}$ are the electric-field amplitudes; ω_X and ω_L are the central frequencies of the two pulses; τ_X is the XUV pulse duration defined as the full width at half maximum (FWHM) and τ_L are the IR laser full pulse duration; and t_d is the time delay between the two pulses, and it is positive if the IR pulse arrives after the XUV pulse.

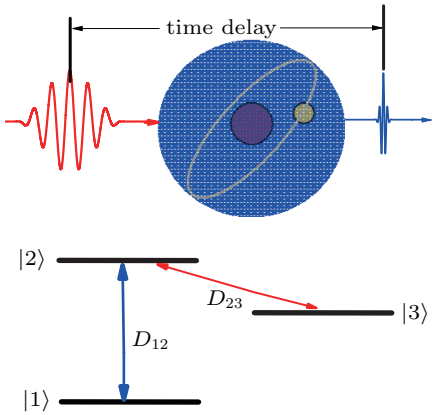


Fig. 1. (color online) Three-level system configuration scheme of the attosecond transient absorption spectroscopy.

The energy levels of helium atom can be obtained by solving the time-independent Schrödinger equation through the generalized pseudospectral method.[24] In order to understand the physical mechanism and simplify the calculation, we consider an three-level atomic system including the states $|1\mathrm{s}\rangle$, $|2\mathrm{p}\rangle$, and $|2\mathrm{s}\rangle$. In three-level model system, the ground state $|1\rangle$, two excited states $|2\rangle$ and $|3\rangle$ stand for the states $|1\mathrm{s}\rangle$, $|2\mathrm{p}\rangle$ and $|2\mathrm{s}\rangle$ of helium atom, respectively (see Fig. 1). The dipole transition is allowed between the states $|1\rangle$ and $|2\rangle$, $|2\rangle$ and $|3\rangle$. For the helium atom, the energy difference Δ_{12} between the states $|1\rangle$ and $|2\rangle$ is 21.01 eV, the energy difference Δ_{23} between the states $|2\rangle$ and $|3\rangle$ is 0.82 eV. The dipole matrix elements between the states $|1\rangle$ and $|2\rangle$ is $D_{12} = 0.38$ a.u. and the dipole matrix elements between the states $|2\rangle$ and $|3\rangle$ is $D_{23} = 2.72$ a.u., both of which are obtained by solving the Schrödinger equation of helium atom. For the one-photon absorption process, because the ground state $|1\rangle$ is an even-parity state, the atom can only be excited to odd-parity state $|2\rangle$ by the attosecond XUV pulse. The even-parity states $|3\rangle$ is not occupied after the XUV pulse excitation. The total time-dependent wave function of the system can be written as

$$\Psi(t) = C_1(t)\,\mathrm{e}^{-\mathrm{i}\varepsilon_1 t}|1\rangle + C_2(t)\,\mathrm{e}^{-\mathrm{i}\varepsilon_2 t}|2\rangle + C_3(t)\,\mathrm{e}^{-\mathrm{i}\varepsilon_3 t}|3\rangle, \tag{4}$$

where ε_1 is the ground-state energy; ε_2 and ε_3 are the energy of the excited states $|2\rangle$ and $|3\rangle$. Inserting the wave function $\Psi(t)$ into the TDSE (Eq. (1)), then

$$\mathrm{i}\frac{\mathrm{d}}{\mathrm{d}t}\begin{bmatrix} C_1 \\ C_2 \\ C_3 \end{bmatrix} = \begin{bmatrix} 0 & H_{12} & 0 \\ H_{21} & 0 & H_{23} \\ 0 & H_{32} & 0 \end{bmatrix}\begin{bmatrix} C_1 \\ C_2 \\ C_3 \end{bmatrix}, \tag{5}$$

H_{21} and H_{32} are the complex conjugate of the H_{12} and H_{23}, respectively.

Model (i) We consider the routinely used three-level model[22,25] and RWA is only used for the interaction between system and IR laser, the fast oscillating term is neglected. In this case, XUV pulse only couples the ground state $|1\rangle$ and the excited state $|2\rangle$, IR pulse couples the two excited states $|2\rangle$ and $|3\rangle$. Suppose their energy levels and the external fields are arranged in such a way that the XUV is near resonance between $|1\rangle$ and $|2\rangle$, then

$$H_{12} = -\mathrm{e}^{-\mathrm{i}\Delta_{12}t} D_{12} E_\mathrm{X}(t,t_\mathrm{d}), \tag{6}$$

$$H_{23} = -\frac{1}{2}\mathrm{e}^{\mathrm{i}\delta_{23}t} D_{23} E_{\mathrm{L}0} f(t), \tag{7}$$

where $\delta_{23} = \omega_\mathrm{L} - \Delta_{23}$.

Model (ii) We also consider the routinely used three-level model,[22,25] but the fast oscillating term is not neglected and RWA is not used. In this case, XUV pulse also only couples the ground state $|1\rangle$ and the excited state $|2\rangle$, IR pulse couples the two excited states $|2\rangle$ and $|3\rangle$

$$H_{12} = -\mathrm{e}^{-\mathrm{i}\Delta_{12}t} D_{12} E_\mathrm{X}(t,t_\mathrm{d}), \tag{8}$$

$$H_{23} = -\mathrm{e}^{-\mathrm{i}\Delta_{23}t} D_{23} E_\mathrm{L}(t). \tag{9}$$

Model (iii) In the routinely used three-level model mentioned above, the IR laser influence on the ground state is not

taken into account, and the RWA neglects the fast oscillating term. In this model, we consider the IR effect on the ground state, and all the coupling mechanism is taken into account.

$$H_{12} = -\mathrm{e}^{-\mathrm{i}\Delta_{12}t} D_{12}[E_{\mathrm{X}}(t,t_{\mathrm{d}}) + E_{\mathrm{L}}(t)], \tag{10}$$

$$H_{23} = -\mathrm{e}^{-\mathrm{i}\Delta_{23}t} D_{23}[E_{\mathrm{X}}(t,t_{\mathrm{d}}) + E_{\mathrm{L}}(t)]. \tag{11}$$

2.2. Calculation of absorption cross section

In general, the transient absorption spectrum is used to describe the atom response to the external field. The weak XUV pulse induces a time-dependent dipole moment in the atom dressed by the IR field, which in turn results in a dipole emission that coherently contributes to the XUV field. For a dilute gas, the relative change of the spectral intensity of the XUV pulse can be expressed in terms of an effective transient absorption atomic cross section $\sigma(\omega)$,[26,27]

$$\sigma(\omega) = -4\pi\alpha\omega \mathrm{Im}\left[\frac{\tilde{d}(\omega)}{\tilde{E}(\omega)}\right], \tag{12}$$

where α is the fine structure constant, $\tilde{E}(\omega)$ represents the Fourier transformation of the XUV field, and $\tilde{d}(\omega)$ denotes the Fourier transformation of the time-dependent dipole moment the time-dependent dipole moment $d(t)$

$$d(t) = \langle \Psi(t)|\boldsymbol{r}|\Psi(t)\rangle. \tag{13}$$

3. Results and discussion

3.1. A direct comparison between different models

In this section, we will discuss the differences among the different models. In the calculation, the XUV pulse duration of FWHM $\tau_{\mathrm{X}} = 200$ attosecond (as), central photon energy $\omega_{\mathrm{X}} = 21$ eV, peak intensity is 10^{10} W/cm^2. The IR laser peak intensity is 10^{12} W/cm^2, central photon energy ω_{L} is 0.6 eV. The full pulse duration τ_{L} of the IR pulse is 20 optical cycle (a long IR laser with narrower bandwidth).

Firstly, we fixed the time delay between the XUV pulse and the IR pulse as four optical cycle (about 27 fs), the XUV pulse is centered at -27 fs and IR pulse is centered at 0 fs. The XUV pulse excites the electron to the excited state $|2\rangle$ from the ground state $|1\rangle$ by one-photon transition. We compare the results based on different models. Figure 2 shows the population and dipole moment based on different models, when the atom interacts with the XUV pulse, state $|2\rangle$ is populated but state $|3\rangle$ still remains zero. As IR pulse comes, states $|2\rangle$ and $|3\rangle$ are coupled and the Rabi cycling among them is observed, after the interaction of the IR pulse, both of them are populated. It is important to note that there are little oscillations in Fig. 2(b) compared to Fig. 2(a), which attributed to the fast oscillating term neglected in RWA. IR laser can lead to the fast oscillation in the population of state $|2\rangle$ when the XUV pulse and IR laser temporally overlaps, which is mainly attributed to the IR laser coupling of state $|2\rangle$ and state $|3\rangle$. However, there are no fast oscillations in Figs. 2(a) and 2(b), compared with Fig. 2(c). The XUV pulse induces a fast oscillating dipole moment, as IR pulse interacts with the system, the fast oscillating dipole moment is modified severely when the XUV pulse and IR laser temporally overlaps, the dipole moment in Figs. 2(d)–2(f) evolve in similar tendency, but there are big differences compared with each other during the XUV pulse and IR laser temporally overlaps. when the XUV pulse and IR laser is turned off, the dipole moment does not exhibit obvious differences among different models.

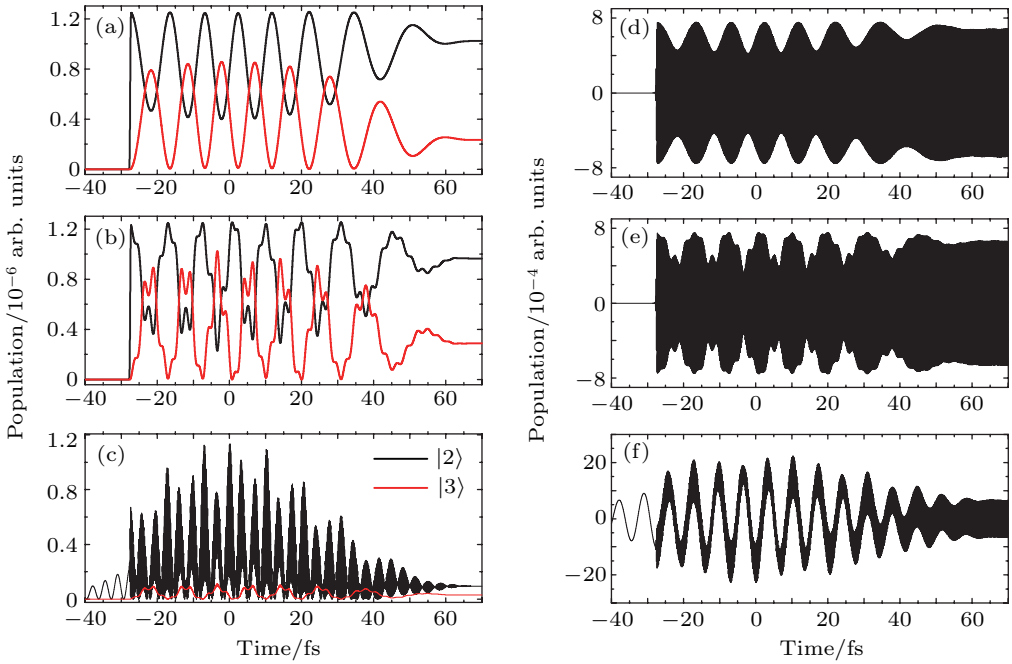


Fig. 2. (color online) The population (a)–(c) and dipole moment (d)–(f) based on different models. (a) and (d) are based on model (i); (b) and (e) are based on model (ii), (c) and (f) are based on model (iii).

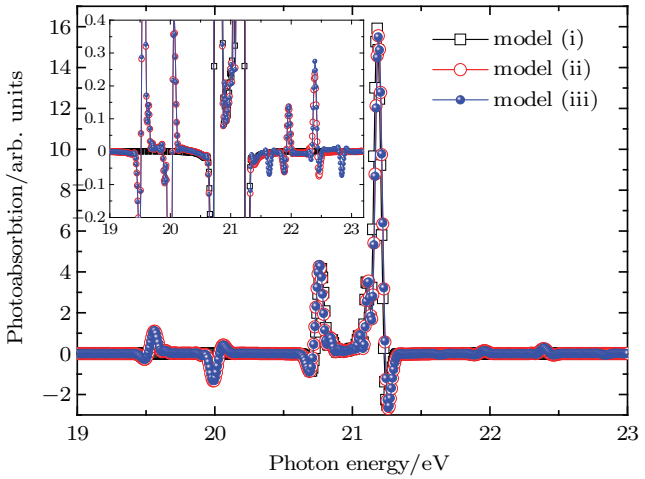


Fig. 3. (color online) Attosecond transient absorption spectroscopy of XUV pulse, which are calculated from the dipole moment shown in Figs. 2(d)–2(f). The insert is an enlarge of the photoabsorbtion spectrum.

As for the transient absorption spectrum, figure 3 shows the same principal peak corresponding to the state $|3\rangle$ which corresponds to the one-photon absorbtion process. However, there are no side peaks in the model (i), but the side peaks are observed in the cases based on the model (ii) and (iii), it is demonstrated that the fast oscillating term neglected in RWA plays an important role in the emergence of the side peaks. Furthermore, the photoabsorbtion based on the model (iii) shows more side peaks than the results based on the model (ii) in the inserted figure, the side peaks at 21.6 eV and 22.8 eV are only observed in the model (iii).

3.2. Attosecond transient absorption spectroscopy in the presence of an IR laser

In this section, we will compare the photoabsorption spectra based on different models in detail and discuss the differences in the presence of an IR laser. The photoabsorption spectra of XUV light in three-level model versus time delay between the XUV pulse and the IR laser are shown in Fig. 4. The overall shape of the photoabsorption spectrum corresponding to the state $|2\rangle$ near 21 eV agrees very well among the different models, but the interference structure misses in Fig. 4(a). As can be seen in Fig. 4, for the case that the IR pulse arrives before the XUV pulse, i.e., at large negative time delays, the main absorbtion line corresponding to state $|2\rangle$ in photoabsorption spectrum exhibits the same features and displays the characteristic Lorentz profiles as if there is only an XUV pulse. By contrast, the main absorbtion line is strongly modified in the presence of the IR pulse near temporal overlap with the XUV pulse: a shifting, splitting and broadening of the main absorption lines can be clearly observed when the IR and XUV pulses overlap in time. This is induced by the strong coupling of the excited states and multiple Rabi cycling between the states $|2\rangle$ and $|3\rangle$. For the case of large positive time delays, the spectrum converges again to the XUV-only case. Furthermore, the fringes around the main absorption lines can also be observed. All of these agree very well with the recent research.[10,14] However, when the XUV pulse and IR laser temporally overlaps and IR laser behind the XUV pulse, the region above and below the main absorbtion line, some stripes and fast oscillations can be observed across the delay scan in Figs. 4(b) and 4(c), which cannot be observed in Fig. 4(a). This means the stripes and fast oscillations are contributed by fast oscillating term neglected by the RWA. The fast oscillating stripes below the main absorbtion line are stronger than that above the main absorbtion line, which is mainly attributed to the three-level model configuration through our multiple calculation.

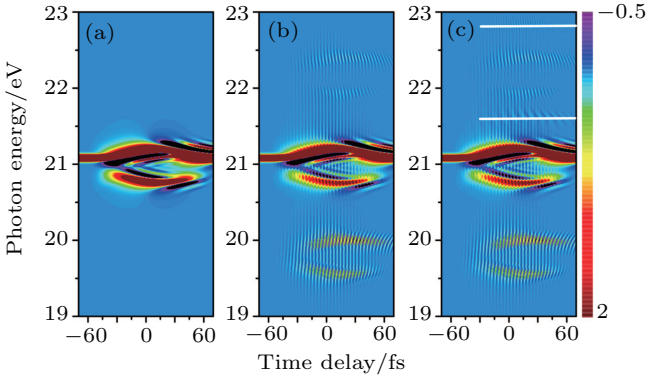


Fig. 4. (color online) Attosecond transient absorption spectroscopy of XUV light in three-level system. (a), (b), and (c) are calculated based the model (i), (ii), and (iii), respectively.

The absorbtion sideband corresponding to the line of $|2\rangle \pm 2\omega_L$, $|3\rangle \pm \omega_L$, and $|3\rangle \pm 3\omega_L$ due to the dipole selection rule, is observed in Figs. 4(b) and 4(c). However, there are more oscillating stripes in Fig. 4(c) (marked by the white solid line) near 22.8 eV and 21.6 eV, which cannot be observed in Fig. 4(b), which suggests that model (ii) neglects some physical information and model (iii) seizes the basic essence. The absorption spectroscopy are fourier transformed along the time delay axis and shown in Fig. 5, the half-cycle modulation frequency of $2\omega_L$ (1.2 eV) are observed in both Figs. 5(a) and 5(b) corresponding to the position of $|2\rangle \pm 2\omega_L$ and $|3\rangle \pm \omega_L$, $|3\rangle \pm 3\omega_L$, even the $4\omega_L$ (2.4 eV) Fourier frequency is also observed. All of these are the same as reported in Ref. [10]. Besides these Fourier frequencies, some new FFT frequencies (0.45 eV, 1.65 eV) are observed in Fig. 5(b), but we cannot observe them in Fig. 5(a). In order to understand these frequency, we transformed the states population based on the model (iii) along the time axis by FFT. Obviously, there are complicated frequency distribution in the population FFT frequency when the IR dressing effect between the ground state $|1\rangle$ and the state $|2\rangle$ is taken into account, and the multiple frequency mixture induces the oscillating stripes in Fig. 4(c) (marked by the white solid line) near 22.8 eV and 21.6 eV, and the FFT frequencies (0.45 eV, 1.65 eV) reflect the results displayed in Fig. 6.

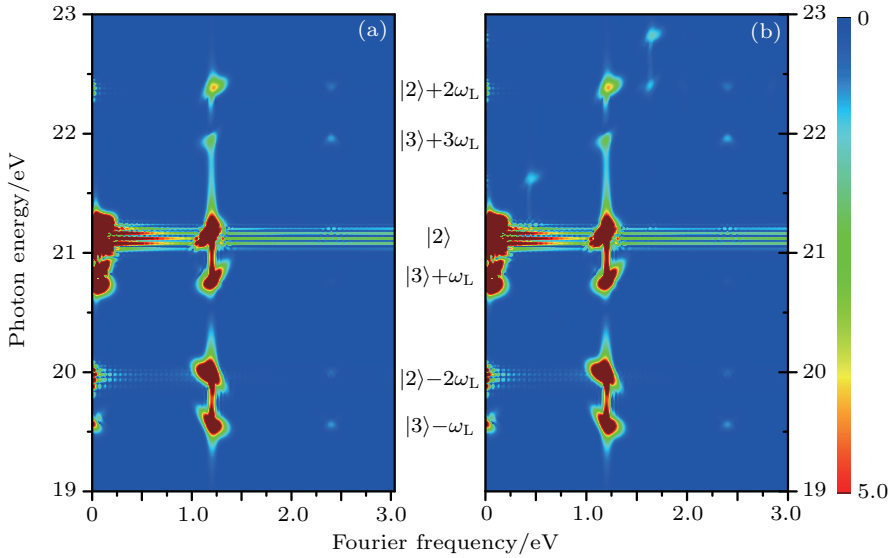


Fig. 5. (color online) Fourier transformation of attosecond transient absorption spectroscopy along the time delay axis. (a) and (b) are the results based on Figs. 4(b) and 4(c), respectively.

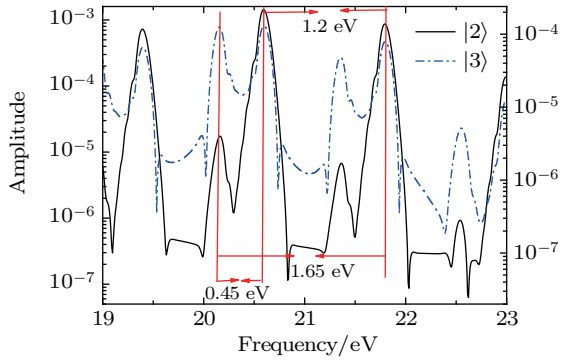


Fig. 6. (color online) Fourier transformation of population based on model (iii).

4. Conclusion

In this paper, time-resolved transient absorption spectroscopy of helium atoms are studied by numerically solving the time-dependent Schrödinger equation (TDSE) numerically based on three-level modeling. The atom is subjected to an XUV pulse and a time-delayed IR laser, we find that three-level model with rotating-wave approximation (RWA) only demonstrates the main absorbtion line corresponding to the one-photon absorbtion process, but can not repeat the fast oscillation structure observed in previous experimental measurements. Three-level model without RWA can show the main features observed in the previous studies, but lost some dressing effect by the IR laser, However, the photoabsorption spectrum based on our modified three-level model (including IR effect on ground state) exhibits more interferences induced by the multiple frequencies mixture. All of these may provide helpful understanding for the XUV absorption spectroscopy.

Acknowledgment

We are grateful to Prof. Liu Jie for the stimulating and fruitful discussions.

References

[1] Krausz F and Ivanov M Y 2009 *Rev. Mod. Phys.* **81** 163
[2] Li F, Wei L and He Z C 2015 *Chin. Phys. B* **24** 043301
[3] Yao T, Jiang W C, Wu P and Peng L Y 2016 *Chin. Phys. B* **25** 073202
[4] Goulielmakis E, Loh Z H, Wirth A, Santra R, Rohringer N, Yakovlev V S, Zherebtsov S, Pfeifer T, Azzeer A M, Klinget M F, Leone S R and Krausz F 2010 *Nature* **466** 739
[5] Wirth A, Hassan M T, Grgura I, Gagnon J, Moulet A, Luu T T, Pabst S, Santra R, Alahmed Z A and Azzeeret A M 2011 *Science* **334** 195
[6] Drescher M, Hentschel M, Kienberger R, Uiberacker M, Yakovlev V, Scrinzi A, Westerwalbesloh T, Kleineberg U, Heinzmann U and Krausz F 2002 *Nature* **419** 803
[7] Wang H, Chini M, Chen S, Zhang C H, He F, Cheng Y, Wu Y, Thumm U and Chang Z 2010 *Phys. Rev. Lett.* **105** 143002
[8] Gilbertson S, Chini M, Feng X, Khan S, Wu Y and Chang Z 2010 *Phys. Rev. Lett.* **105** 263003
[9] Chini M, Zhao B, Wang H, Cheng Y, Hu S X and Chang Z 2012 *Phys. Rev. Lett.* **109** 073601
[10] Chen S M, Bell J, Beck A R, Mashiko H, Wu M, Pfeiffer A N, Gaarde M B, Neumark D M, Leone S R and Schafer K J 2012 *Phys. Rev. A* **86** 063408
[11] Chen S, Wu M, Gaarde M B and Schafer K J 2012 *Phys. Rev. A* **87** 033408
[12] Chini M, Wang X, Cheng Y, Wu Y, Zhao D, Telnov D A, Chu S and Chang Z 2013 *Sci. Rep.* **3** 1105
[13] Pfeiffer A N and Leone S R 2012 *Phys. Rev. A* **85** 053422
[14] Wu M, Chen S, Gaarde M and Schafer K 2013 *Phys. Rev. A* **88** 043416
[15] Wang X W, Chini M, Cheng Y, Wu Y, Tong X M and Chang Z 2013 *Phys. Rev. A* **87** 063413
[16] Ott C, Kaldun A, Raith P, Meyer K, Laux M, Evers J, Keitel C H, Greene C H and Pfeifer T 2013 *Science* **340** 716
[17] Ott C, Kaldun A, Argenti L, Raith P, Meyer K, Laux M, Zhang Y Z, Blättermann A, Hagstotz S, Ding T, Heck R, Madroñ ero J, Martín F and Pfeifer T 2014 *Nature* **516** 374
[18] Chu W C and Lin C D 2012 *Phys. Rev. A* **85** 013409
[19] Argenti L, Ott C, Pfeifer T and Martín F 2012 arXiv:1211.2566
[20] Yang Z Q, Ye D F, Ding T, Pfeifer T and Fu L B 2015 *Phys. Rev. A* **91** 013414
[21] Yang Z Q and Zhang L D 2015 *Acta Phys. Sin.* **64** 133203 (in Chinese)
[22] Chu W C, Zhao S F and Lin C D 2011 *Phys. Rev. A* **84** 033426
[23] Fano U 1961 *Phys. Rev.* **124** 1866
[24] Tong X M and Chu S I 1997 *Chem. Phys.* **217** 119
[25] Cai X, Zhao J, Wang Z and Lin Q 2013 *J. Phys. B* **46** 175602
[26] Gaarde M B, Buth C, Tate J L and Schafer K J 2011 *Phys. Rev. A* **83** 013419
[27] Santra R, Yakovlev V S, Pfeifer T and Loh Z H 2011 *Phys. Rev. A* **83** 033405